ORIGINAL ARTICLE

🔓 OPEN ACCESS

Novel conformation-specific monoclonal antibodies against amyloidogenic forms of transthyretin

Jeffrey N. Higaki[1], Avi Chakrabartty[2], Natalie J. Galant[2], Kevin C. Hadley[2], Bradley Hammerson[3], Tarlochan Nijjar[1], Ronald Torres[1], Jose R. Tapia[1], Joshua Salmans[1], Robin Barbour[1], Stephen J. Tam[1], Ken Flanagan[1], Wagner Zago[1], and Gene G. Kinney[1]

[1]Prothena Biosciences Inc, South San Francisco, CA, USA, [2]Princess Margaret Cancer Centre, University Health Network, Toronto, Ontario, Canada, and [3]Seattle Genetics, Bothell, WA, USA

Abstract

Introduction: Transthyretin amyloidosis (ATTR amyloidosis) is caused by the misfolding and deposition of the transthyretin (TTR) protein and results in progressive multi-organ dysfunction. TTR epitopes exposed by dissociation and misfolding are targets for immunotherapeutic antibodies. We developed and characterized antibodies that selectively bound to misfolded, non-native conformations of TTR.

Methods: Antibody clones were generated by immunizing mice with an antigenic peptide comprising a cryptotope within the TTR sequence and screened for specific binding to non-native TTR conformations, suppression of *in vitro* TTR fibrillogenesis, promotion of antibody-dependent phagocytic uptake of mis-folded TTR and specific immunolabeling of ATTR amyloidosis patient-derived tissue.

Results: Four identified monoclonal antibodies were characterized. These antibodies selectively bound the target epitope on monomeric and non-native misfolded forms of TTR and strongly suppressed TTR fibril formation *in vitro*. These antibodies bound fluorescently tagged aggregated TTR, targeting it for phagocytic uptake by macrophage THP-1 cells, and amyloid-positive TTR deposits in heart tissue from patients with ATTR amyloidosis, but did not bind to other types of amyloid deposits or normal tissue.

Conclusions: Conformation-specific anti-TTR antibodies selectively bind amyloidogenic but not native TTR. These novel antibodies may be therapeutically useful in preventing deposition and promoting clearance of TTR amyloid and in diagnosing TTR amyloidosis.

Abbreviations: ATTR, transthyretin amyloid protein; D, non-native dimer; Fmoc, fluorenyl-methyloxycarbonyl; K_D, equilibrium dissociation constant; LC, light chain; M, monomer; mAbs, monoclonal antibodies; MAP, multiple antigenic peptide; ND, native dimer; O, oligomer; pAb, polyclonal antibody; PBS, phosphate-buffered; SPR, surface plasmon resonance; T, tetramer; TTR, transthyretin

Introduction

Amyloidoses are progressive diseases characterized by the accumulation of amyloid fibrils originating from a variety of different precursor proteins in multiple organs throughout the body, leading to organ dysfunction and death [1]. The most common hereditary form of this disease is transthyretin amyloidosis (ATTR amyloidosis), caused by the accumulation of the plasma protein transthyretin (TTR) [2]. Hereditary ATTR amyloidosis is an autosomal dominant and incompletely penetrant disease. It is classified by the specific TTR mutation and is associated with cardiac involvement and neuropathic involvement [3,4]. Hereditary ATTR amyloidosis is caused by the presence of one of more than 100 known point mutations in the TTR gene that produces TTR isoforms having a higher propensity for aggregation and fibril formation than the wild-type protein [5,6]. A second nonhereditary, sporadic form of ATTR amyloidosis, wild-type ATTR amyloidosis, is associated primarily with cardiac deposition of wild-type TTR in the heart and occasional TTR amyloid in carpal tunnel ligaments [7,8]. ATTR amyloidoses are age-associated (onset typically at >60 years) and lead to progressive, systemic illness and death, with mean life expectancies of 5–6 years with cardiomyopathy and 9–11 years with non-cardiac pathology [9]. Current therapies include liver

transplantation to remove the primary source of circulating, mutant TTR in hereditary ATTR amyloidosis [10] and treatment with agents such as tafamidis meglumine [11,12] or diflunisal [13] designed to kinetically stabilize the TTR tetramer, delaying its dissociation into potentially amyloidogenic monomers. Several treatments are currently in clinical development that aim to reduce amyloid deposition by lowering *de novo* TTR production in the liver [14,15] and thereby prevent TTR fibril formation, deposition and/or enhance clearance [16]. There are no approved treatments that directly clear deposited TTR amyloid to potentially reverse organ dysfunction.

TTR is a 55 kDa homotetrameric protein that transports thyroxin and vitamin A, the latter via an interaction with vitamin-A bound retinol-binding-protein [17]. The TTR tetramer is composed of four 127 amino acid, 14 kDa single-chain monomers with a dimer-of-dimers assembly. However, under conditions that destabilize the TTR tetramer (denaturation with low pH and/or elevated temperature, or the presence of familial point mutations), the tetrameric protein can more readily dissociate, leading to a conformational change of free monomers that favors aggregation and fibril formation [18,19].

A potential treatment for the diseases characterized by amyloid deposition involves the use of monoclonal antibodies (mAbs) that selectively bind the dissociated monomers, non-native oligomers and/or aggregates to prevent fibril formation, or that bind the amyloid deposits themselves, targeting them for removal by phagocytic mechanisms [20,21]. Targeting all these pathogenic forms with a single antibody, while sparing the normal tetrameric TTR, is also conceivable. For TTR, such an immunotherapeutic mechanism could supplement the native immune system's ability to produce antibodies against non-native forms of TTR, thereby delaying or preventing the onset of disease symptoms [22,23]. In addition, preclinical research demonstrating that active immunization of TTR-V30M transgenic mice (mice expressing human TTR containing a common ATTR amyloidosis-associated mutation) with the aggregation-prone TTR variant TTR-Y78F reduced TTR-V30M deposition and induced the production of non-native TTR antibodies [24]. These findings prompt the idea that conformation-specific antibodies with selectivity for non-native TTR species may be therapeutically beneficial if administered passively.

Previously described TTR epitopes unique to non-native forms of TTR, which distinguish native from misfolded TTR [24–30], may be suitable targets for misfolded TTR-specific antibodies. Based on a structural analysis of the TTR tetramer in comparison to the structure of the monomer, Bugyei-Twum et al. (manuscript submitted) identified a novel cryptotope, comprising residues 89–97. This epitope is sequestered at the dimer interfaces of the tetrameric protein but is exposed upon tetramer dissociation and subsequent misfolding of the released monomers into amyloidogenic precursors [Bugyei-Twum et al., submitted]. A polyclonal antibody (pAb) against this cryptotope specifically bound to non-native, misfolded forms of TTR and prevented amyloid formation at substoichiometric levels, suggesting that this epitope might be a critical nucleation site for aggregation and fibril formation [Bugyei-Twum et al., submitted]. In addition, this pAb

selectively immunolabeled TTR amyloid in tissue from patients with ATTR amyloidosis, confirming the non-native structure of TTR present in amyloid as suggested by Gustavsson et al. [25]. The objective of the present study was to produce mAbs specific for this unique epitope, to establish their utility in preventing TTR fibril formation and promoting cellular uptake of aggregated TTR *in vitro* and to demonstrate binding to TTR deposits in tissue from patients with ATTR amyloidosis. Such mAbs could potentially be used therapeutically to prevent TTR deposition and/or enhance TTR amyloid clearance in patients with ATTR amyloidosis, either alone or in combination with other therapeutic strategies.

Methods

Recombinant TTR

Escherichia coli (BL21-A1) cells were transformed with a pET21a(+) plasmid containing either the TTR insert Met-hTTR-His6 (tetrameric wild-type TTR), the destabilized variants of TTR associated with familial ATTR amyloidosis (TTR-V122I and TTR-V30M) [31] or the monomeric TTR-F87M/L110M [32]. Transformed cells were grown in 2YT broth (100 μg/mL ampicillin). Plasmid expression was induced overnight (20 °C, 1 mM isopropyl β-D-1-thiogalacto-pyranoside, 0.05% arabinose), and cells were centrifuged (4000 × g, 10 min) and stored at −80 °C. Thawed pellets (10–15 g) were lysed with Buffer A (50 mL 1× phosphate-buffered saline (PBS), 500 mM NaCl, 20 mM imidazole) using an LV-1 high-shear processor (Microfluidics, Inc., Westwood, MA), centrifuged (27 000 × g; 30 min; 4 °C), filtered (0.2 μm PES filter) and purified on a His-Trap HP column (GE Life Sciences, Pittsburgh, PA), washed (10 column volumes of Buffer A) and eluted with Buffer B (1 × PBS, 500 mM NaCl, 500 mM imidazole). TTR fractions were dialyzed against 1 × PBS and stored at −80 °C.

Production of TTR fibrils

Thioflavin-T–positive TTR fibrils were generated by exposure of tetrameric TTR to low pH conditions for extended periods of time to allow for tetramer dissociation and fibril formation. This was accomplished by diluting recombinant TTR to a final concentration of 0.2 mg/mL (3.6 μM) in 50 mM sodium acetate pH 4 and incubating at room temperature for 72 h. Fibril formation was monitored with thioflavin-T fluorescence (5-fold molar excess, 30 min; excitation wavelength, 442 nm; emissions wavelength, 482 nm) using a Paradigm Imager (Paradigm, Houston, TX) and by native PAGE. The resulting fibrillar TTR sample (pH4-TTR) was stored at 4 °C.

Low pH-aggregated TTR-V30M for the cell-based phagocytosis assay was produced as follows: purified TTR-V30M protein was diluted to 2.0 mg/mL in 50 mM sodium phosphate and titrated to pH 2.7 with citric acid. The sample was placed in a Thermomixer (Eppendorf AG) at 37 °C, 500 rpm for 2 weeks. Aggregated, thioflavin-T–positive protein was collected by centrifugation at 100 000 × g for 1 h, and the resulting clear, gelatinous pellet was washed once with 1 × PBS, then thoroughly resuspended in 1 × PBS to a final concentration of 2.0 mg/mL.

Antibody generation and hybridoma selection

A multiple antigenic peptide (MAP) with the TTR89–97 sequence flanked by glycine linkers (ggEHAEVVFTAggkg) was synthesized on a [Fluorenylmethyloxycarbonyl (Fmoc) Fmoc-Lys (Fmoc)] 4-Lys2-Lys-bAla-Wang resin using Fmoc-protected amino acids, as described above (Bugyei-Twum et al., submitted). Additional immunogens were generated by covalently linking TTR89–97 peptides (Ac-cggEHAEVVFTA-amide and Ac-EHAEVVFTAggc-amide) via the N- and C-terminal cysteine residues to keyhole limpet hemocyanin (TTR89–97-N-KLH and TTR89–97-C-KLH). Mice were immunized with the antigenic peptides (RIBI adjuvant weekly or in TiterMax adjuvant monthly), with a final immunogen boost 3–4 d prior to fusion. Homogenized spleens were fused with SP2/0 myeloma cells, plated and screened after 7–10 d. Hybridomas were selected based upon specific binding to non-native pH4-TTR using a sandwich ELISA and goat anti-mouse (IgG1, 2a, 2b, 3 specific)-HRP (1:5000, 0.5% BSA/PBS/ TBS-T). After 3 d of growth, clones were counter-screened with native TTR to eliminate non-discriminating clones.

Antibody expression and purification

Hybridoma cells were expanded in shake flasks and seeded into 10–25 L Wave bag cultures (CD hybridoma expression media with Glutamax [Life Technology]). Batch cultures were prepared using a Wave Bioreactor (GE Healthcare, Piscataway, NJ; 37 °C, 7% CO_2 under constant agitation) with periodic cell number monitoring. Cultures were harvested when cell viability declined below 50% (5–7 d), clarified through a depth filter (Millistak Pod COHC; Millipore, Billerica, MA), sterile filtered (0.2 µm filter; Optican XL; Millipore), concentrated 10-fold by tangential flow filtration (Pelicon 2PLC 30K, Millipore) and then sterile filtered (0.2 µm filter; PES Filter System; Corning).

Concentrated conditioned media were loaded onto a pre-equilibrated Protein G Sepharose Fast Flow column (GE Life Sciences; 1 × PBS, pH 7.4, Akta Avant FPLC) and washed (5–10 column volumes, 1 × PBS, pH 7.4) until the OD_{280} reached baseline. Bound antibody was eluted with 2 column volumes of IgG Elution Buffer (Thermo Scientific, Grand Island, NY) and pH neutralized (2M tris, pH 9.0, 60 µL/mL). Antibody-containing fractions were pooled and dialyzed overnight (4 °C; 1 × PBS; pH 7.4), sterilized by ultrafiltration (0.2 µm PES filter) and stored at 4 °C. The final protein concentration was determined by bicinchoninic acid using a bovine gamma-globulin standard (Thermo Scientific).

Surface plasmon resonance

Anti-mouse antibodies (anti-mouse kit; GE Healthcare) were immobilized on a CM5 sensor chip per manufacturer's instructions. Antibodies were captured at levels to ensure binding of 30–50 response units of analyte (TTR F87M/ L110M). Three-fold analyte dilutions in running buffer (HEPES-buffered saline, 0.05% P-20, 1 mg/mL BSA) were passed over the captured ligand at a flow rate of 30 µL/min, spanning a concentration range at least 10-fold above K_D to 10-fold below K_D, based on preliminary studies. The reaction duration was optimized to allow for equilibrium to be reached during the association phase with 10% signal decay during dissociation for each analyte concentration. At least one mid-range concentration was run in duplicate. All surface plasmon resonance (SPR) measurements were performed on a Biacore T200 (GE Healthcare).

SDS- and native-PAGE electrophoresis and Western blot analysis

SDS-PAGE gels

A 0.1–1 µg sample of TTR or pH4-TTR in lithium dodecyl sulfate sample buffer (Life Technologies) was run on a 10% NuPAGE bis-tris gel (MES buffer; 90 V, 105 min) and stained with Instant Blue (Expedeon, San Diego, CA) or transferred to nitrocellulose membranes for Western blot analysis.

Native-PAGE tris-glycine gels

A 0.1–1 µg sample of TTR or pH4-TTR in 1× tris-glycine sample buffer (Life Technologies) was run on an 8–16% tris-glycine native gel (120 V, 105 min) and stained or transferred to nitrocellulose membranes.

Western blot analysis

Nitrocellulose transfers (iBlot, Life Technologies) were treated with blocking buffer (LI-COR, Lincoln, NE) and incubated in 0.50 µg/mL primary antibody, washed with 1× TBS and placed in 1:20 000 dilution of IRDye 800CW-conjugated goat-anti-mouse secondary antibody (LI-COR), then imaged on an Odyssey CL× infrared imager (LI-COR).

TTR fibril inhibition assay

A stock solution of TTR-V122I (approximately 5 mg/mL) was diluted into buffer with final concentrations of 0.2 mg/mL TTR, 30 mM sodium acetate, 5 mM sodium phosphate, 100 mM KCl, 1 mM EDTA, 0.02% sodium azide, and varying concentrations of mAb at pH 7.2. This sample was dialyzed against the same buffer at pH 4.5 for 3 h at room temperature. Samples were then incubated at 37 °C for 72 h. The extent of fibril formation was probed by Thioflavin T (ThT) (Sigma-Aldrich, St Louis, MO). A five-fold molar excess of ThT was added to each sample and left at room temperature for 30 min before measurements were taken. ThT fluorescence was monitored using a Photon Technology International C60 spectrofluorometer. The photomultiplier gain was varied and excitation and emission slit widths set to 2–4 nm to maximize signal to noise. Fluorescence measurements were made using 430 and 480 nm as excitation and emission wavelengths, respectively.

The ThT fluorescence was normalized with the following formula to enable comparison of fluorescence measurements taken on different days:

$$\text{Normalized fluorescence} = \frac{\left(\begin{array}{c} \text{Observed ThT fluorescence} \\ - \text{ fluorescence of ThT in buffer} \end{array} \right)}{\left(\begin{array}{c} \text{fluorescence of ThT in 0.2 mg/mL aggregated} \\ \text{V122I} - \text{TTR} - \text{fluorescence of ThT in buffer} \end{array} \right)}$$

Table 1. Antibodies used for immunohistochemistry.

Antibody	Antibody type	Vendor	Catalog number	Concentration
6F10	Isotype Control	Prothena Biosciences	–	0.5 µg/mL
Prealbumin	Total-TTR	Dako North America	A0002	1:2000 & 1:20 000
Kappa light chains	AL-κ	Dako North America	A0191	1:8000
Lambda light chains	AL-λ	Dako North America	A0193	1:8000
Amyloid A	AA	Dako North America	M0759	1:8000

Phagocytosis assay

pHrodo dye-labeling of TTR

A 1 mg/mL sample of TTR-F87M/L110M, native TTR or low-pH aggregated TTR-V30M was amine coupled with pHrodo dye for 15 min at 37 °C with a protein:dye ratio of ≈15:4 according to the manufacturer's specifications (Thermo Scientific). Excess pHrodo-label was removed by diafiltration in a spin concentrator with a 10 K molecular weight cutoff (Pierce Thermo) and the pHrodo-TTR was resuspended in 1 × PBS.

Phagocytosis assay

THP-1 human monocytes were cultured in cell culture media (RPMI, 10% low IgG serum, pen/strep). A 20 µg/mL aliquot of pHrodo-labeled TTR was separately pre-incubated with 40 µg/mL antibody at 37 °C in cell culture media for 30 min prior to the addition of 5E + 04 THP-1 cells in a 1:1 volumetric ratio. After tissue culture incubation (3 h), cells were washed with cell culture media three times, incubated in media for 10 min, then washed twice with and resuspended in FACS buffer (1% FBS in PBS). Red pHrodo fluorescence intensity was detected using Texas Red channel filters. Epifluorescence microscopy was carried out in a similar fashion. After FACS analysis, the remaining cells were transferred to glass chamber slides and imaged by inverted microscopy. Mean fluorescence intensities were automatically calculated by averaging the relative fluorescence intensities of each individual cell.

Histology and imaging

Human tissue samples

Fresh frozen and paraffin-processed cardiac tissue with confirmed genetic and/or histopathological diagnoses of hereditary and sporadic ATTR cardiac amyloidosis and amyloid light chain (AL) amyloidosis were generously donated by Dr. Merrill Benson (Indiana University, Indianapolis, IN). Fresh frozen normal control heart, liver and pancreas were procured from Bioreclamation IVT (Baltimore, MD) and a matching paraffin set of tissue was obtained from American MasterTech (Lodi, CA). Paraffin sections of normal human choroid plexus were purchased from Biochain (Newark, CA).

Immunohistochemistry

Lightly paraformaldehyde-fixed, slide-mounted cryosections (10 µm) and paraffin sections (5 µm) were immunoperoxidase labeled on the Leica Bond Rx with the polymer detection kit (DS980, Leica Biosystems, Buffalo Grove, IL). Antibody reagents used for immunohistochemistry are listed in Table 1. After primary incubation (1 h) and anti-mouse or anti-rabbit polymeric HRP-linker antibody-conjugates incubation, staining was visualized with diaminobenzidine. Labeling specificity was assessed by staining cardiac tissue from normal and AL amyloidosis patients (negative controls). Reagent controls included performing the staining procedure on adjacent slides with non-immune isotype control (6F10) primary antibodies and omitting the primary antibodies altogether.

Demonstration of amyloid and typing

Amyloid was labeled using a Congo red kit (American MasterTech) per manufacturer's instructions and a filtered 0.015% thioflavin T (T3516–25G; Sigma-Aldrich; 50% ethanol, 10 min) [33]. The specific type of amyloid deposited in the tissue was identified by IHC using a panel of commercial antibodies to TTR (prealbumin), λ light chains, κ light chains, and serum amyloid A (Table 1).

Image analysis

Slides were imaged with an Olympus BX61 microscope equipped with a 10×/0.40 and a 20×/0.75 UPlanSApo objective (Central Valley, PA). Congo red-stained slides were evaluated between a crossed polarizer and analyzer for the characteristic apple-green birefringence of amyloid deposits while thioflavin T fluorescence was visualized using appropriate filters. Whole slides were digitally scanned using a Hamamatsu Nanozoomer 2.0HT digital slide scanner (Hamamatsu, Bridgewater, NJ).

Results

Generation of conformation-specific mis-TTR mAbs

We previously described the production and characterization of a conformation-specific mis-TTR pAb that selectively binds monomeric or misfolded conformations of TTR and inhibits TTR fibril formation *in vitro* but does not recognize native tetrameric TTR (Bugyei-Twum et al., submitted). This pAb was generated using a MAP antigen containing residues 89–97 of TTR chosen on the basis of a structural analysis of tetrameric TTR versus the monomeric, dissociated monomer [29]. Residues 89–97 (EHAEVVFTA; Figure 1A) are located within the F strand of TTR and sequestered at the dimer interface of the tetrameric protein, but they are exposed upon tetramer dissociation and thus constitute a cryptotope (Figure 1B). A BLAST search of the protein database did not reveal any other human proteins possessing this sequence (Bugyei-Twum et al., submitted).

We used a similar approach to generate mis-TTR mAbs. We synthesized a peptide having the sequence

(A)

```
  1- GPTGTGESKCPLMVKVLDAVRGSPAINVAVHVFRKAADDT - 40
 41- WEPFASGKTSESGELHGLTTEEEFVEGIYKVEIDTKSYWK - 80
 81- ALGISPFHEHAEVVFTANDSGPRRYTIAALLSPYSYSTTA - 120
121- VVTNPKE - 127
```
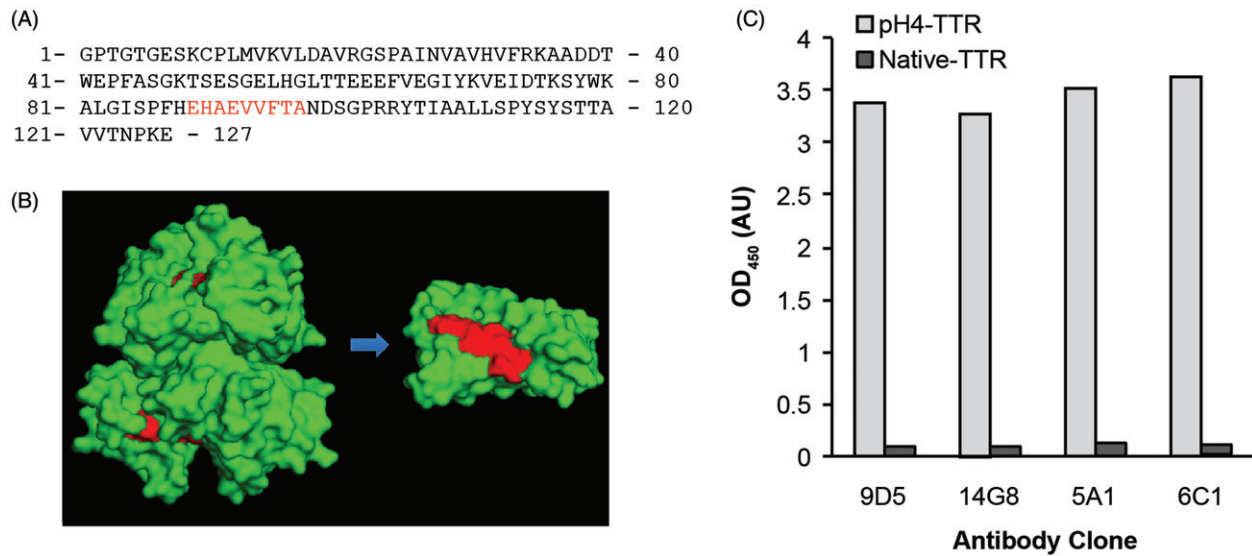
(B)

(C)

Figure 1. Generation of conformation-specific mis-TTR mAbs. (A) The amino acid sequence of human TTR highlighting the location of the mis-TTR epitope (residues 89–97, red). (B) Location of the mis-TTR epitope (red), which is inaccessible to mis-TTR mAb binding due to its location within the tetramer (left), but is exposed in the dissociated monomer (right). (C) The primary sandwich ELISA screening assay identified four clones that reacted strongly against pH4-TTR (light gray bars) and with minimal reactivity toward native, tetrameric TTR (dark gray bars).

ggEHAEVVFTAggkg linked to a poly-lysine dendritic core, which generated a MAP immunogen comprising a core of lysine residues with multiple branches linked to the TTR 89–97 peptide. This peptide sequence, ggEHAEVVFTAggkg, included TTR residues 89–97 (capital letters) with additional linker residues (lowercase) that were added to increase the solubility of the antigenic peptide and to establish the nine amino acid TTR epitope as an internal sequence.

In addition to this MAP, two other immunogens containing the same nine amino acid TTR epitope were generated by covalently linking the TTR 89–97 peptides (Ac-cggEHAEVVFTA-amide and Ac-EHAEVVFTAggc-amide), via their N- and C-terminal cysteine residues, to keyhole limpet hemocyanin (TTR89–97-N-KLH and TTR89–97-C-KLH). Immunization of mice with these MAP antigens resulted in the production of four unique high-titer hybridoma clones (9D5, 14G8, 6C1 and 5A1) that were chosen based on initial ELISA screening results for strong reactivity toward pH4-TTR with little/no reactivity toward native, tetrameric TTR (Figure 1C). The isotypes of these four mouse mAbs were determined as follows: 9D5 and 14G8 (IgG1/κ); 6C1 (IgG2a/κ); 5A1 (IgG2b/κ).

Conformational specificity of mis-TTR mAbs

The conformational specificity of the four mis-TTR mAbs identified in the primary screen was further explored by non-denaturing SDS-PAGE and Western blot analysis. Separation of native TTR by non-denaturing SDS-PAGE and staining with Instant Blue showed the presence of a ∼38 kDa native dimer (ND) with a very small amount of native tetramer (T) (Figure 2A). pH4-TTR (F) migrated as primarily a 15 kDa monomer (M) and a ∼37 kDa dimer (D). A close inspection of the dimer bands observed in the native TTR versus pH4-TTR samples showed that the ∼37 kDa pH4-TTR dimer (D) migrated slightly faster than the native TTR dimer (ND), indicating that these dimers were not the same species.

Analysis of this non-denaturing SDS-PAGE gel by Western blot using the four mis-TTR mAbs showed that these antibodies identified both the monomer (M) and non-native dimer (D) bands present in the pH4-TTR sample, but did not recognize either the native tetramer (T) or the native dimer (ND) species (Figure 2A). In contrast, neither 8C3 (a mAb raised against fully denatured TTR) nor the Sigma pAb discriminated between native and non-native TTR species (Figure 2B).

The specificity of mis-TTR mAbs for non-native conformations of TTR was further investigated by native PAGE/Western blot analysis (Figure 2C). Separation of native TTR on a native gel showed the presence of the ∼60 kDa native tetramer (T) and a small amount of a high-molecular weight native oligomer (O) when stained with Instant Blue. Both of these species were identified by the Sigma pAb, but not by any of the mis-TTR mAbs. In contrast, pH4-TTR (F) migrated as a high molecular weight smear ranging from ≈80 to ≈480 kDa in size and showed strong reactivity with all four mis-TTR mAbs, indicating that the pH4-TTR sample was composed largely of non-native TTR aggregates. In contrast, the Sigma pAb did not discriminate between native and non-native TTR species, reacting with both the native tetramer (T) and the native oligomer (O) along with the high molecular weight non-native smear present in the pH4-TTR sample.

The kinetic parameters for each antibody binding to misfolded TTR were determined by SPR analysis using TTR-F87M/L110M. This TTR variant contains a double mutation at amino acid residues 87 and 110 of TTR that disrupts monomer-monomer contacts required for native tetramer assembly [32]. Unlike misfolded, aggregated pH4-TTR, TTR-F87M/L110M yielded a more homogeneous, mostly monomeric preparation of misfolded TTR as determined by gel filtration chromatography (data not shown) that was more suitable for SPR analysis. The kinetic parameters for binding of each of the four mis-TTR mAbs to monomeric TTR-F87M/L110M are shown in Table 2. All four mis-TTR
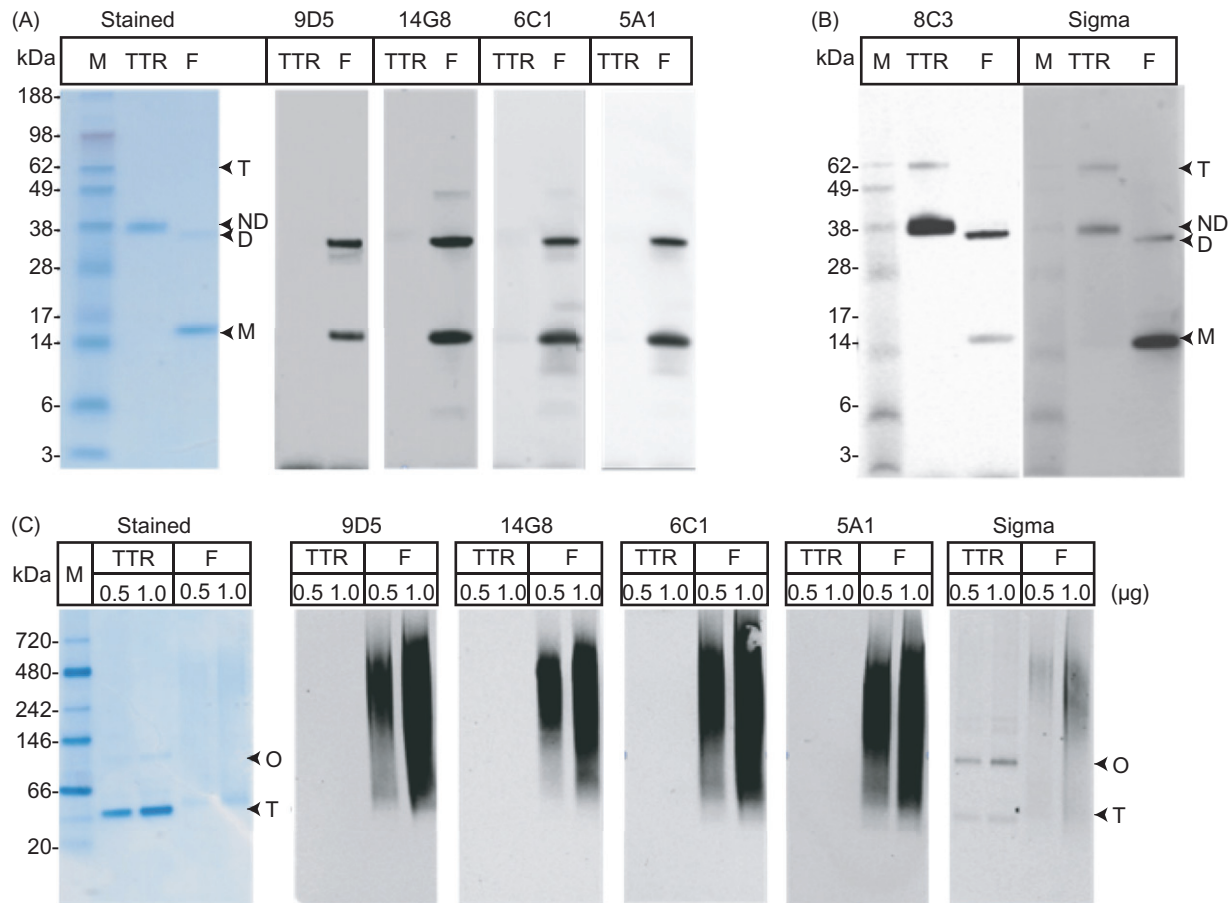
Figure 2. Characterization of mis-TTR mAbs by Western blot analysis. (A) Native TTR (TTR) and pH4-TTR (F) were separated by non-denaturing SDS-PAGE and stained with instant blue or Western blotted with mis-TTR mAbs. Under these PAGE conditions, native TTR migrated as primarily an ~38 kDa native dimer (ND) with a minor amount of ~60 kDa tetramer (T). pH4-TTR migrated as an ~15 kDa monomer (M) and a ~32 kDa non-native dimer (D). All four mis-TTR mAbs showed immunoreactivity toward the non-native TTR monomer and dimer, but did not react with native TTR. (B) In contrast, the total TTR mAbs, 8C3 and the Sigma pAb did not discriminate between TTR species. (C) By native-PAGE/Western, native TTR migrated as a tetramer (T) and a higher molecular weight native oligomer (O) while pH4-TTR (F), composed of aggregated forms of TTR, migrated as a high molecular weight smear ranging in size from ~66–720 kDa. All four mis-TTR mAbs strongly recognized this high molecular weight TTR smear but did not react with the native tetramer or native oligomer. In contrast, the Sigma pAb reacted with all TTR species and did not show any conformational specificity.

Table 2. Kinetic parameters for binding of mis-TTR antibodies to TTR-F87M/L110M determined by SPR.

Mis-TTR mAb	k_a (1/Ms)	k_d (1/s)	K_D (M)	R_{max}
9D5	2.71E+04	4.93E−04	1.82E−08	31.55
14G8	2.88E+04	5.36E−04	1.86E−08	37.13
5A1	6.11E+04	4.69E−04	7.68E−09	30.98
6C1	4.61E+04	4.15E−04	9.01E−09	26.32

k_a, association rate constant; k_d, dissociation rate constant; K_D, equilibrium dissociation constant; R_{max}, maximum response.

mAbs showed nanomolar affinities for this TTR variant. Additionally, similar maximum response values among the four antibodies indicated uniform saturation binding to TTR-F78M/L110M.

Inhibition of TTR fibril formation

We evaluated the ability of the mis-TTR mAbs to inhibit TTR fibril formation at substoichiometric ratios, as previously demonstrated with the mis-TTR pAbs (Bugyei-Twum et al.,

submitted). For these studies, TTR-V122I, a TTR variant containing a single V122I amino acid substitution that destabilizes the tetramer, making it more prone to aggregation and fibril formation [31], was exposed to mildly acidic incubation conditions that favored fibril formation yet maintained antibody binding activity. Fibril formation was associated with an increase in ThT fluorescence (Figure 3).

Increasing 14G8 mAb concentrations caused a monotonic decrease in ThT fluorescence indicating a substoichiometric inhibition of TTR fibrillation (IC$_{50}$ = 0.028 ± 0.009 mg/mL; $n = 3$; Figure 3A and Table 3). The isotype control mAb did not cause inhibition of TTR fibrillation (Figure 3B), thus demonstrating the specificity of 14G8 mediated inhibition. The isotype control data were more variable than the 14G8 data, which is likely a result of the stochastic nature of aggregation that produces variability in the size and number of aggregates formed. This variability decreased in the presence of inhibitory antibodies. Similar observations have been reported with inhibitors of aggregation of the brain protein, TDP-43 [34].

Comparable substoichiometric IC$_{50}$ values determined for 5A1 and 6C1 (Table 3) suggested analogous mechanisms of
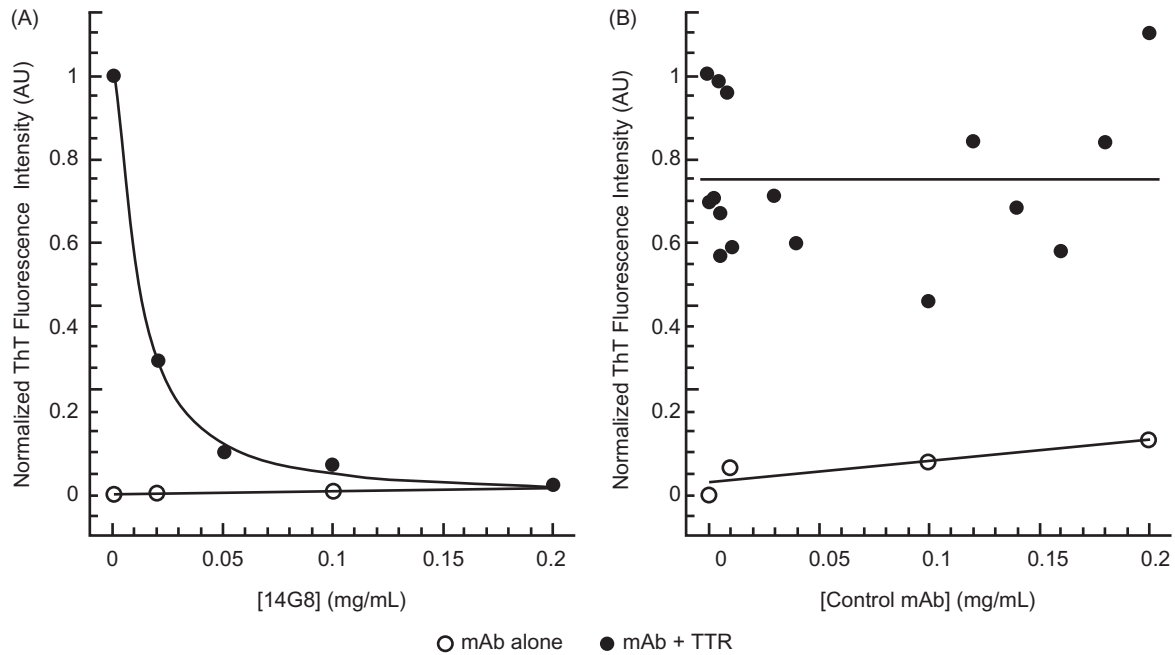
Figure 3. Inhibition of TTR-V122I fibril formation by mis-TTR mAbs. (A) TTR fibril formation (induced by incubation of TTR-V122I at pH 4.8 for 72 h and assessed by end-point thioflavin-T (ThT) fluorescence) was inhibited in the presence of 0–0.2 mg/mL 14G8 mis-TTR mAb (filled circles). Antibody alone (open circles) exhibited very little ThT binding and fluorescence. (B) In contrast to 14G8, the isotype control antibody, EG27/1, did not inhibit TTR fibril formation as demonstrated by no reduction in ThT fluorescence intensity.

Table 3. Inhibition of TTR-V122I fibril formation by mis-TTR antibodies ($n=3$ assays/antibody).

Antibody	IC$_{50}$±SD mg/mL)
9D5	No inhibition
14G8	0.028 ± 0.009
6C1	0.048 ± 0.059
5A1	0.015 ± 0.02
EG 27/1	No inhibition

fibril inhibition for each of these mis-TTR mAbs. In contrast, 9D5 unexpectedly failed to inhibit TTR-V122I fibril formation, despite showing similar specificity and affinity for non-native TTR. It remains to be explored whether 9D5 is more sensitive to the assay conditions used (e.g. low pH).

Antibody-dependent uptake of TTR by THP-1 cells

To determine whether these mis-TTR-specific antibodies can promote the *in vitro* uptake of non-native TTR by human monocyte phagocytosis, TTR-F87M/L110M was covalently labeled with the pH-sensitive fluorescent dye pHrodo; the pHrodo tag has minimal fluorescence under physiological pH, but fluorescence is enhanced upon engulfment into the low pH environments of endocytic vesicles and thus marks cellular uptake of tagged particles. THP-1 monocytes were added to pHrodo-tagged TTR (native or non-native, TTR-F87M/L110M) after treatment with either 14G8 or the isotype control antibody. Low levels of fluorescence were observed with either antibody incubated with native TTR, and after incubation of the control antibody with non-native TTR. Fluorescence was increased after 14G8 incubation with non-native TTR (Figure 4A), suggesting that non-native TTR is

not efficiently phagocytized under basal conditions; however, the addition of mis-TTR antibodies specifically elicits phagocytosis of non-native TTR.

Dose-dependent phagocytosis of pHrodo-labeled, large aggregated fibrillar particles of TTR was also demonstrated for each of the mis-TTR mAbs (Figures 4B and 4C). Maximum antibody-dependent uptake was variable for each mis-TTR mAb (6C1 > 9D5 ≈ 14G8 > 5A1), reaching a plateau at mAb concentrations between 5–10 μg/mL. Variable antibody potencies may reflect isotype differences and associated changes in effector function among the four mis-TTR mAbs. Controls, including untreated cells or those treated with an IgG1 isotype control, did not demonstrate detectable or enhanced fluorescence, respectively. These data support the concept that mis-TTR antibodies can elicit clearance of extracellular soluble and insoluble aggregates of non-native TTR by opsonization and subsequent phagocytosis.

Immunohistochemical evaluation of mis-TTR mAbs

We examined whether the mis-TTR mAbs could specifically immunolabel TTR amyloid deposits in cardiac tissue from patients with I84S ATTR mutation. 14G8 and total-TTR immunoreactivities (Figures 5A and 5B) were overlapping and identified comparable deposits intercalated between the cardiomyocytes and in the vasculature that were not immunoreactive for 6F10, an IgG1 isotype control antibody (Figure 5C). These same deposits were also labeled by thioflavin T (Figure 5D) and Congo red (Figures 5E and 5F), which confirm their amyloid nature. Less intense 14G8 immunoreactivity (Figure 5A, arrows) was also found in regions not staining for amyloid, and thus may represent staining of pre-amyloid TTR deposits.
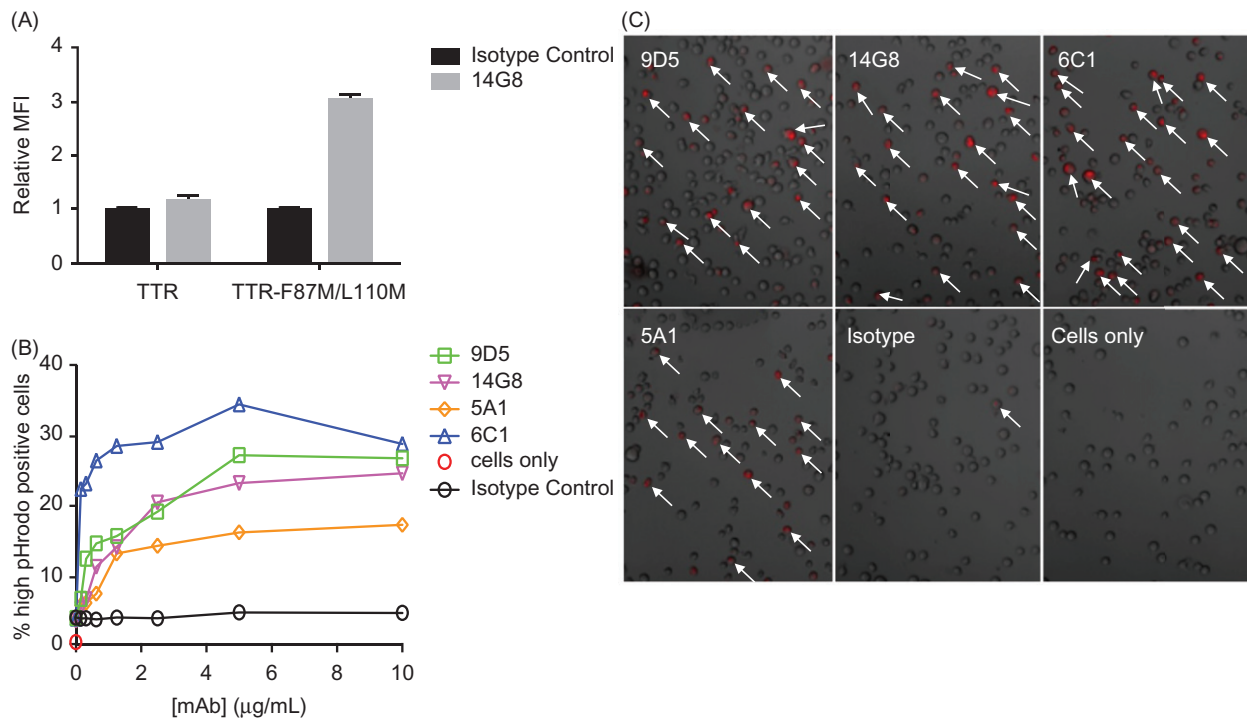
Figure 4. mis-TTR mAb-dependent phagocytosis. (A) TTR-F87M/L110M or native TTR was covalently labeled with the pH-sensitive fluorescent dye, pHrodo, which shows enhanced fluorescence upon exposure to lowered pH in endocytic vesicles. Uptake of the pHrodo label as measured by relative mean fluorescence intensity (MFI) of THP-1 cells was specific for pHrodo-TTR-F87M/L110 that was treated with 14G8 (gray bars), but not an isotype control antibody (black bars). 14G8 had no effect on the uptake of native pHrodo-TTR. Data are presented as mean ± SEM ($n=3$). (B) All four anti-mis-TTR antibodies increased uptake of aggregated pHrodo-ATTR V30M in a dose-dependent fashion as measured by pHrodo-positive THP-1 cells. In contrast, no uptake was observed in cells treated with an isotype control IgG and no fluorescence was detected in untreated cells (red circle). (C) Representative 20× objective pHrodo 594 brightfield overlays of THP-1 cells showing uptake of aggregated pHrodo-TTR-V30M in the presence of mis-TTR antibodies (most intensely fluorescent pHrodo-positive THP-1 cells denoted with white arrows).
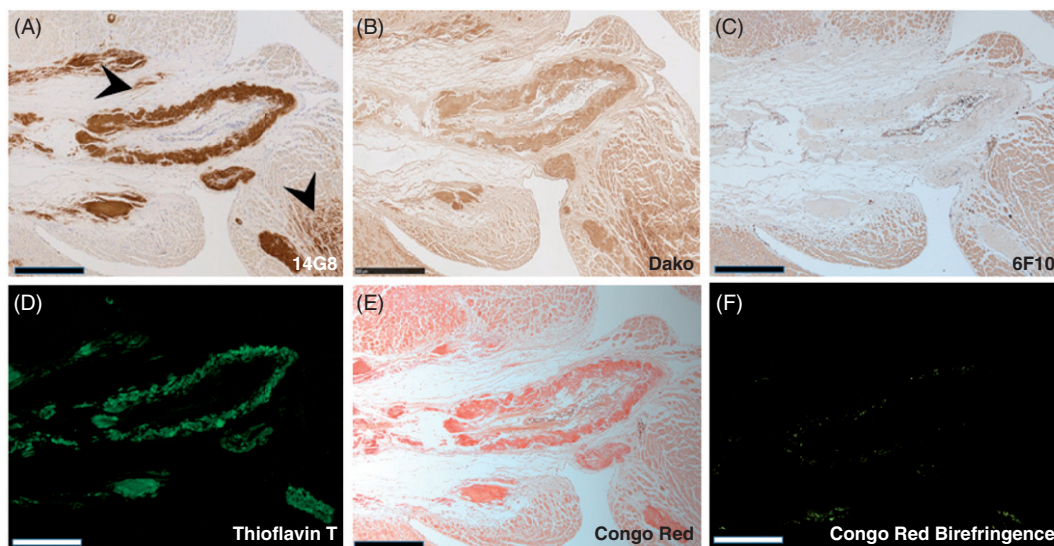

Figure 5. 14G8 specifically identifies amyloidogenic TTR deposits in human ATTR amyloidosis cardiac tissue. Immunohistochemical labeling of cardiac tissue derived from an ATTR amyloidosis patient harboring the I84S mutation. (A) 14G8 mis-TTR mAb and (B) total-TTR pAb (DAKO) immunoreactivities were overlapping and identified comparable deposits in the myocardium and vasculature that were not immunoreactive for anti-6F10 (C), an isotype control. Lower-intensity immunohistochemical labeling with 14G8 (black arrows, A) was found in regions not staining for amyloid, and thus may represent pre-amyloidogenic TTR deposits. These same deposits were also labeled by thioflavin T (D) and Congo red (E), which confirmed the amyloid nature of these deposits. Congo red birefringence (F) aligned with the same areas showing the greatest amount of TTR deposits. Scale bar = 500 μm.

Specific and intense 14G8 staining was also observed in heart tissue samples taken from ATTR amyloidosis patients harboring various TTR mutations (V122I, T60A, T49A and I84S) or wild-type ATTR amyloidosis (Figure 6A). Similar specific immunolabeling was also observed with the other three mis-TTR mAbs (9D5, 6C1 and 5A1; Supplementary Figures 1–3). The specificity of mis-TTR immunolabeling was further confirmed by a complete absence of reactivity in
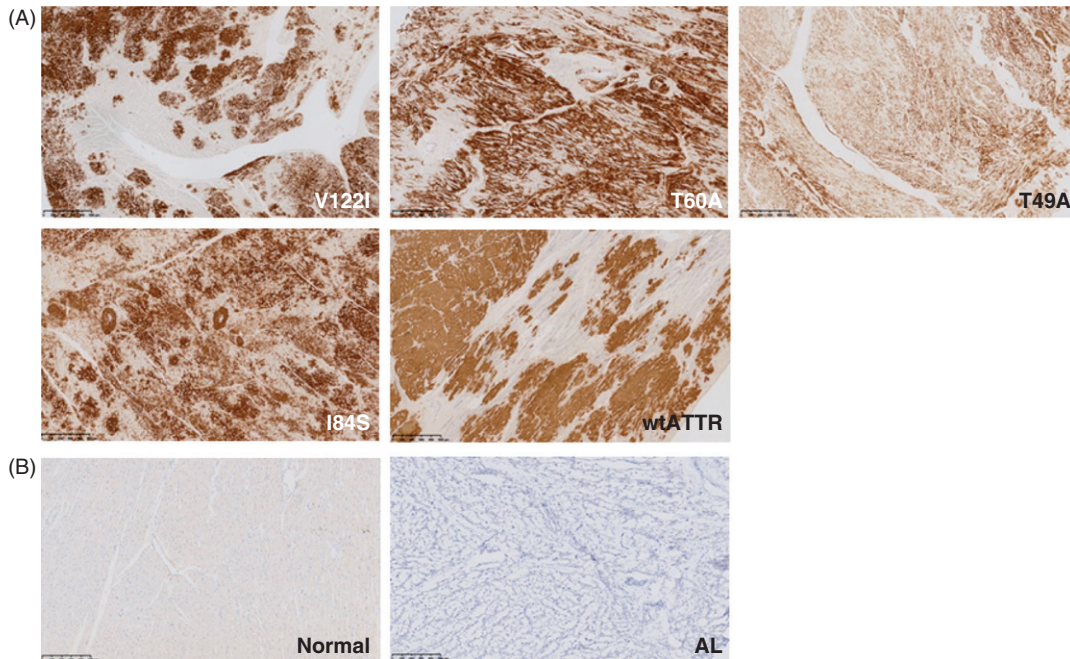
Figure 6. 14G8 immunolabels cardiac tissue from patients with hereditary and sporadic ATTR amyloidosis cardiomyopathy. (A) 14G8 strongly immunolabeled TTR deposits in diseased ATTR amyloidosis heart tissue derived from patients with familial (V122I, T60A, T49A, I84S) and wild-type forms of cardiac ATTR amyloidosis. (B) No 14G8 immunolabeling was observed in cardiac tissue from healthy individuals (Normal) or from cardiomyopathy patients with non-related AL amyloidosis (AL). Scale bar = 500 μm.
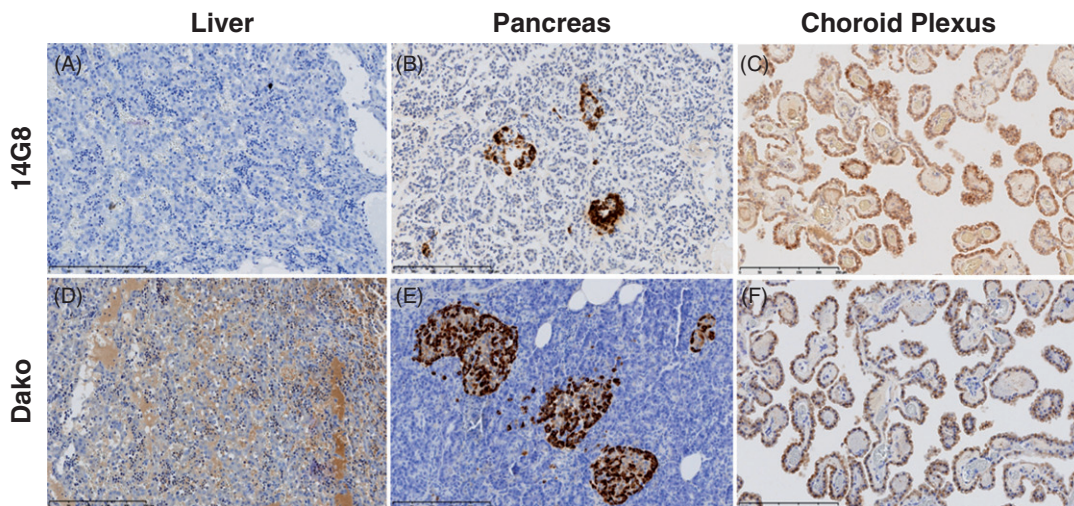

Figure 7. Staining of TTR by the 14G8 mis-TTR mAb in normal tissue known to express TTR. 14G8 did not stain the TTR present in normal human liver (A) but did stain intracellular TTR present in normal pancreatic α-cells (B) and choroid plexus (C) from normal donors. Staining of tissue with 14G8 was specific as demonstrated by the lack of staining in adjacent sections using an isotype control antibody (data not shown). This is in contrast to staining of TTR using the Dako antibody which stained total TTR present in all three of these normal tissue types (D–F). Scale bar = 250 μm.

cardiac tissue derived from healthy individuals without ATTR amyloidosis and from patients with primary AL amyloidosis, another form of amyloidosis with cardiac deposits (Figure 6B).

We examined mis-TTR immunolabeling in the normal liver, pancreatic α-cells and the choroid plexus, organs known to express and secrete TTR. 14G8 specifically labeled the TTR present in pancreatic α-cells and the modified ependymal cells of the choroid plexus, but not the TTR present in normal human liver (Figure 7). In contrast, intense immunolabeling was observed in all this tissue using the total anti-TTR antibody (Dako; Figures 7D–F). This finding was expected since the TTR present in this tissue is native,

tetrameric TTR. The ability of 14G8 and other mis-TTR mAbs (see Supplementary Figure 4) to recognize TTR produced in the pancreas and choroid plexus but not in the liver suggests that some of the TTR produced in the pancreas and choroid plexus may be structurally distinct from that produced in the liver, possibly a result of different cellular or tissue environments.

Discussion

We used a rational, structure-based approach to generate mAbs that selectively target a TTR cryptotope, composed of

residues 89–97, which is exposed only in monomers and non-native conformations of TTR. ELISA, Western blot and SPR analysis confirmed that mis-TTR mAbs bind with a high affinity to non-native forms of TTR but do not bind to native, tetrameric TTR in which the 89–97 epitope is inaccessible. This feature allows mis-TTR mAbs to target TTR amyloid or TTR species involved in the amyloidogenic process while sparing the function of the native protein in thyroxin and vitamin A transport.

TTR fibrillogenesis is thought be initiated by the dissociation of the native tetramer into constituent monomeric subunits, followed by a conformational change that initiates a nucleation-dependent polymerization process, similar to that observed for other amyloidogenic proteins [35,36]. Stable, self-organized nuclei are expanded by the sequential addition of monomeric intermediates to form fibrils. The rate of nucleation-dependent polymerization can be coupled with cellular injury and death [35], and thus it may be an important therapeutic target.

The ability of mis-TTR antibodies to suppress fibrillogenesis *in vitro* at substoichiometric levels suggests that the TTR amyloidogenic species targeted by mis-TTR mAbs, although very impactful, may be at low abundance in relation to the total TTR in solution. Binding to these precursors likely sequesters them from the amyloidogenic pathway, preventing nucleation and further aggregation and fiber formation. Alternatively, the antibodies may present a catalytic activity, where their binding to TTR aggregates could disrupt the tertiary structure, resulting in disaggregation. This phenomenon, described as catalytic disaggregation, was demonstrated previously for anti-amyloid beta protein antibodies [37]. Although studies are currently under way to determine the precise mechanism by which mis-TTR mAbs inhibit TTR aggregation and fibril formation, the mis-TTR epitope we describe here spans the aggregation-prone region within the F-strand of TTR that was recently found to be directly involved in the TTR aggregation process [38]. Thus, it is likely that our mis-TTR mAbs inhibit TTR aggregation and fibril formation by impeding the self-association of the protein as proposed for small non-native peptides specific for this site [38]. That 9D5 failed to inhibit *in vitro* fibrillogenesis was unexpected since this antibody showed binding affinities and selectivity for non-native conformations of TTR similar to the other three mis-TTR mAbs. This may be due to unique biophysical properties of the antibody (i.e. stability, solubility, or propensity to aggregate) that make it more sensitive to the low pH conditions used in this assay. Further studies are needed to more precisely determine why 9D5 was not active in this assay.

In addition to preventing TTR amyloid fibril formation, mis-TTR mAbs might also have utility in clearing previously deposited TTR amyloid present in affected organs through stimulation of antibody-dependent phagocytosis, as reported for antibodies against other amyloidogenic proteins [21,39,40]. Evidence supporting that mis-TTR mAbs may provide this therapeutic advantage comes from *in vitro* experiments demonstrating antibody-dependent phagocytic uptake of soluble and insoluble TTR by human monocytes.

Immunolabeling of amyloid deposits in cardiac tissue from patients with confirmed familial and wild-type ATTR amyloidosis, but not from healthy controls or from patients with AL amyloidosis, demonstrates that the mis-TTR epitope is specific to ATTR amyloidosis. The ability of mis-TTR mAbs to bind to this exposed TTR epitope suggests that other amyloid binding proteins such as serum amyloid P [41] or other post-translationally modified proteins [42] that may also be present do not occlude this TTR amyloid-specific epitope.

The lack of immunolabeling of wild-type TTR in the liver, the primary site of TTR synthesis in humans, indicates that this tissue expresses native, tetrameric TTR, which further supports the hypothesis that mis-TTR mAbs do not target native TTR. However, the significance of mis-TTR mAb binding in the α-cells of the pancreas and in cells from the choroid plexus of healthy individuals remains to be determined. It is possible that this staining may indicate the presence of monomeric or other non-tetrameric conformations of TTR resulting from tissue-specific differences in protein folding and secretion efficiency (e.g., tissue-specific protein chaperones or other binding partners impacting ER processing) [43]. Nevertheless, the mis-TTR mAb staining pattern in the pancreas and the choroid plexus most likely represents TTR that is inaccessible to antibody binding using immunotherapeutic approaches.

Reducing non-tetrameric TTR serum levels in combination with inhibiting TTR nucleation and targeting fibrils for phagocytic clearance may attenuate or block TTR aggregation and improve symptoms in patients. While experiments demonstrating the *in vivo* efficacy of anti-mis-TTR antibodies are beyond the scope of these studies, we reported that another conformational-specific mAb targeting an epitope unique to the misfolded aggregates of the immunoglobulin light chain protein promoted clearance of AL amyloid extracts in a mouse amyloidoma model, likely by engaging phagocytes to clear deposits [21]. Those studies have been translated into clinical trials using similar immunotherapeutic approaches in patients with AL amyloidosis, where we recently reported positive biomarker responses suggestive of improved cardiac and renal function [44] The potential significance of mis-TTR antibodies as immunotherapeutic agents is also supported by specific antibody-mediated approaches for other diseases characterized by amyloidosis [20] and may be useful in combination with other ATTR amyloidosis treatments, such as liver transplantation and/or agents that stabilize TTR tetramers.

In addition to their potential use as immunotherapeutics, mis-TTR mAbs may prove useful in the diagnosis of ATTR amyloidosis if levels of immunoreactive TTR species can be correlated with the disease. Patient sera, cerebrospinal fluid or tissue biopsy specimens may be assayed with mis-TTR mAbs to improve the detection of ATTR amyloidosis, which is believed to be significantly underdiagnosed [45]. Improvements in the speed and accuracy of diagnosis could provide patients earlier access to treatments, potentially intervening prior to significant deterioration in organ function and likely improving patient prognoses. In accord with suspected underdiagnosis of ATTR amyloidosis and wild-type ATTR amyloidosis, such ante- and post-mortem testing could also improve estimates of the prevalence of this disease and may be beneficial in gauging prognosis and treatment response.

Conclusion

In this report, we describe the generation of mAbs (mis-TTR mAbs) that are selective for monomeric, misfolded and amyloidogenic forms of TTR. These antibodies inhibit TTR fibrillogenesis and induce antibody-dependent phagocytic uptake of TTR aggregates *in vitro*. In addition, these antibodies bind specifically to amyloid deposits in cardiac samples derived from patients with several confirmed ATTR mutations, demonstrating the exposure of this epitope in relevant disease tissue. Future studies will assess the pharmacokinetics of mis-TTR mAbs, their penetration and retention in target tissue, and efficacy in animal models, which could determine the diagnostic and therapeutic potential in patients with ATTR amyloidosis.

Acknowledgements

Declaration of interest

References

1. Merlini G, Seldin DC, Gertz MA. Amyloidosis: pathogenesis and new therapeutic options. J Clin Oncol 2011;29:1924–33.
2. Ueda M, Ando Y. Recent advances in transthyretin amyloidosis therapy. Transl Neurodegener 2014;3:19.
3. Sekijima Y. Transthyretin (ATTR) amyloidosis: clinical spectrum, molecular pathogenesis and disease-modifying treatments. J Neurol Neurosurg Psychiatry 2015;86:1036–43.
4. Rowczenio DM, Noor I, Gillmore JD, Lachmann HJ, Whelan C, Hawkins PN, Obici L, et al. Online registry for mutations in hereditary amyloidosis including nomenclature recommendations. Hum Mutat 2014;35:E2403–12.
5. Connors LH, Lim A, Prokaeva T, Roskens VA, Costello CE. Tabulation of human transthyretin (TTR) variants, 2003. Amyloid 2003;10:160–84.
6. Ando Y, Coelho T, Berk JL, Cruz MW, Ericzon BG, Ikeda S, Lewis WD, et al. Guideline of transthyretin-related hereditary amyloidosis for clinicians. Orphanet J Rare Dis 2013;8:31.
7. Westermark P, Sletten K, Johansson B, Cornwell III GG. Fibril in senile systemic amyloidosis is derived from normal transthyretin. Proc. Natl. Acad. Sci. U.S.A. 1990;87:2843–5.
8. Sikora JL, Logue MW, Chan GG, Spencer BH, Prokaeva TB, Baldwin CT, Seldin DC, et al. Genetic variation of the transthyretin gene in wild-type transthyretin amyloidosis (ATTRwt). Hum Genet 2015;134:111–21.
9. Coehlo T, Erikson BG, Falk R, Grogan D, Ikeda SI, Mauer M, Planté-Bordeneuve V, et al. A physician's guide to transthyretin amyloidosis. Amyloidosis Foundation; c2008.
10. Holmgren G, Ericzon BG, Groth CG, Steen L, Suhr O, Andersen O, Wallin BG, et al. Clinical improvement and amyloid regression after liver transplantation in hereditary transthyretin amyloidosis. Lancet 1993;341:1113–16.
11. Bulawa CE, Connelly S, DeVit M, Wang L, Weigel C, Fleming JA, Packman J, et al. Tafamidis, a potent and selective transthyretin kinetic stabilizer that inhibits the amyloid cascade. Proc. Natl. Acad. Sci. U.S.A. 2012;109:9629–34.
12. Coelho T, Maia LF, Martins da Silva A, Waddington CM, Planté-Bordeneuve V, Lozeron P, Suhr OB, et al. Tafamidis for transthyretin familial amyloid polyneuropathy: a randomized, controlled trial. Neurology 2012;79:785–92.
13. Berk JL, Suhr OB, Obici L, Sekijima Y, Zeldenrust SR, Yamashita T, Heneghan MA, et al. Repurposing diflunisal for familial amyloid polyneuropathy: a randomized clinical trial. Jama 2013;310:2658–67.
14. Coelho T, Adams D, Silva A, Lozeron P, Hawkins PN, Mant T, Perez J, et al. Safety and efficacy of RNAi therapy for transthyretin amyloidosis. N Engl J Med 2013;369:819–29.
15. Ackermann EJ, Guo S, Booten S, Alvarado L, Benson M, Hughes S, Monia BP. Clinical development of an antisense therapy for the treatment of transthyretin-associated polyneuropathy. Amyloid 2012;19:43–4.
16. Arsequell G, Planas A. Methods to evaluate the inhibition of TTR fibrillogenesis induced by small ligands. Curr Med Chem 2012;19:2343–55.
17. Kanai M, Raz A, Goodman DS. Retinol-binding protein: the transport protein for vitamin A in human plasma. J Clin Invest 1968;47:2025–44.
18. Jiang X, Buxbaum JN, Kelly JW. The V122I cardiomyopathy variant of transthyretin increases the velocity of rate-limiting tetramer dissociation, resulting in accelerated amyloidosis. Proc Natl Acad Sci USA. 2001;98:14943–8.
19. Kelly JW. Alternative conformations of amyloidogenic proteins govern their behavior. Curr Opin Struct Biol 1996;6:11–17.
20. De Genst E, Messer A, Dobson CM. Antibodies and protein misfolding: from structural research tools to therapeutic strategies. Biochim Biophys Acta 2014;1844:1907–19.
21. Wall JS, Kennel SJ, Williams A, Richey T, Stuckey A, Huang Y, Macy S, et al. AL amyloid imaging and therapy with a monoclonal antibody to a cryptic epitope on amyloid fibrils. PLoS One 2012;7:e52686.
22. Obayashi K, Tasaki M, Jono H, Ueda M, Shinriki S, Misumi Y, Yamashita T, et al. Impact of antibodies against amyloidogenic transthyretin (ATTR) on phenotypes of patients with familial amyloidotic polyneuropathy (FAP) ATTR Valine30Methionine. Clin Chim Acta 2013;419:127–31.
23. Planque SA, Nishiyama Y, Hara M, Sonoda S, Murphy SK, Watanabe K, Mitsuda Y, et al. Physiological IgM class catalytic antibodies selective for transthyretin amyloid. J Biol Chem 2014;289:13243–58.
24. Terazaki H, Ando Y, Fernandes R, Yamamura K, Maeda S, Saraiva MJ. Immunization in familial amyloidotic polyneuropathy: counteracting deposition by immunization with a Y78F TTR mutant. Lab Invest 2006;86:23–31.
25. Gustavsson Å, Engström U, Westermark P. Mechanisms of transthyretin amyloidogenesis. Antigenic mapping of transthyretin purified from plasma and amyloid fibrils and within *in situ* tissue localizations. Am J Pathol 1994;144:1301–11.
26. Redondo C, Damas AM, Saraiva MJM. Designing transthyretin mutants affecting tetrameric structure: implications in amyloidogenicity. Biochem J 2000;348:167–72.
27. Phay M, Blinder V, Macy S, Greene MJ, Wooliver DC, Liu W, Planas A, et al. Transthyretin aggregate-specific antibodies recognize cryptic epitopes on patient-derived amyloid fibrils. Rejuvenation Res 2014;17:97–104.
28. Su Y, Jono H, Torikai M, Hosoi A, Soejima K, Guo J, Tasaki M, et al. Antibody therapy for familial amyloidotic polyneuropathy. Amyloid 2012;19:45–6.
29. Goldsteins G, Persson H, Andersson K, Olofsson A, Dacklin I, Edvinsson Å, Saraiva MJ, et al. Exposure of cryptic epitopes on transthyretin only in amyloid and in amyloidogenic mutants. Proc. Natl. Acad. Sci. U.S.A. 1999;96:3108–13.
30. Redondo C, Damas AM, Olofsson A, Lundgren E, Saraiva MJM. Search for intermediate structures in transthyretin fibrillogenesis: soluble tetrameric Tyr78Phe TTR expresses a specific epitope present only in amyloid fibrils. J Mol Biol 2000;304:461–70.
31. Hurshman Babbes AR, Powers ET, Kelly JW. Quantification of the thermodynamically linked quaternary and tertiary structural stabilities of transthyretin and its disease-associated variants: the

relationship between stability and amyloidosis. Biochemistry 2008; 47:6969–84.

32. Jiang X, Smith CS, Petrassi HM, Hammarström P, White JT, Sacchettini JC, Kelly JW. An engineered transthyretin monomer that is nonamyloidogenic, unless it is partially denatured. Biochemistry 2001;40:11442–52.

33. Schmidt ML, Robinson KA, Lee VM, Trojanowski JQ. Chemical and immunological heterogeneity of fibrillar amyloid in plaques of Alzheimer's disease and Down's syndrome brains revealed by confocal microscopy. Am J Pathol 1995;147:503–15.

34. Sun Y, Arslan PE, Won A, Yip CM, Chakrabartty A. Binding of TDP-43 to the 3'UTR of its cognate mRNA enhances its solubility. Biochemistry 2014;53:5885–94.

35. Wogulis M, Wright S, Cunningham D, Chilcote T, Powell K, Rydel RE. Nucleation-dependent polymerization is an essential component of amyloid-mediated neuronal cell death. J Neurosci 2005;25: 1071–80.

36. Xue W-F, Homans SW, Radford SE. Systematic analysis of nucleation-dependent polymerization reveals new insights into the mechanism of amyloid self-assembly. Proc. Natl. Acad. Sci. U.S.A. 2008;105:8926–31.

37. Solomon B, Koppel R, Frankel D, Hanan-Aharon E. Disaggregation of Alzheimer beta-amyloid by site-directed mAb. Proc Natl Acad Sci USA 1997;94:4109–12.

38. Saelices L, Johnson LM, Liang WY, Sawaya MR, Cascio D, Ruchala P, Whitelegge J, et al. Uncovering the mechanism of aggregation of human transthyretin. J Biol Chem 2015;290: 28932–43.

39. Bard F, Cannon C, Barbour R, Burke R-L, Games D, Grajeda H, Guido T, et al. Peripherally administered antibodies against amyloid β peptide enter the central nervous system and reduce pathology in a mouse model of Alzheimer disease. Nat Med 2000; 6:916–19.

40. Hrncic R, Wall J, Wolfenbarger DA, Murphy CL, Schell M, Weiss DT, Solomon A. Antibody-mediated resolution of light chain-associated amyloid deposits. Am J Pathol 2000;157:1239–46.

41. Pepys MB, Dyck RF, de Beer FC, Skinner M, Cohen AS. Binding of serum amyloid P-component (SAP) by amyloid fibrils. Clin Exp Immunol 1979;38:284–93.

42. Teixeira AC, Saraiva MJ. Presence of N-glycosylated transthyretin in plasma of V30M carriers in familial amyloidotic polyneuropathy: an escape from ERAD. J Cell Mol Med 2013;17:429–35.

43. Sekijima Y, Wiseman RL, Matteson J, Hammarström P, Miller SR, Sawkar AR, Balch WE, et al. The biological and chemical basis for tissue-selective amyloid disease. Cell 2005;121:73–85.

44. Gertz M, Landau H, Comenzo RL, Seldin D, Weiss B, Zonder J, Merlini G, et al. First in human phase I/II study of NEOD001 in patients with light chain amyloidosis and persistent organ dysfunction. J Clin Oncol 2016; [Epub ahead of print]. DOI: 10.1200/JCO.2015.63.6530.

45. Ruberg FL, Berk JL. Transthyretin (TTR) cardiac amyloidosis. Circulation 2012;126:1286–300.

Supplementary materials available online